Trajectory Studies of S_N2 Nucleophilic Substitution. 4. Intramolecular and Unimolecular Dynamics of the Cl^----CH_3Br and $ClCH_3$---Br^- Complexes

Haobin Wang, Gilles H. Peslherbe, and William L. Hase*

Contribution from the Department of Chemistry, Wayne State University, Detroit, Michigan 48202

Received May 12, 1994®

Abstract: Classical trajectory calculations, performed on an analytic potential energy function derived from *ab initio* calculations, are used to study the intramolecular and unimolecular dynamics of the Cl^----CH_3Br complex with initial mode specific excitation. Two distinct patterns are observed in the dynamics of this complex. When the low-frequency modes are excited, the complex preferentially dissociates to $Cl^- + CH_3Br$. However, when the high-frequency CH_3Br intramolecular modes are excited, the above is a negligible reaction path and, instead, Cl^----$CH_3Br \rightarrow ClCH_3$---$Br^-$ becomes important. Contrary to RRKM theory, the $ClCH_3$---Br^- complexes formed by this isomerization do not immediately dissociate to $ClCH_3 + Br^-$ but remain trapped in the central barrier region of the potential energy surface, with extensive barrier recrossings. The intramolecular dynamics of Cl^----CH_3Br and $ClCH_3$---Br^- are interpreted in terms of intermolecular and intramolecular complexes, with the former accessing the dissociation products and the latter the central barrier region. There is a dynamical bottleneck for transitions between these two complexes. The $ClCH_3 + Br^-$ product energies, for $ClCH_3$---Br^- complexes which do dissociate, are in agreement with the previous experimental study of Graul and Bowers [*J. Am. Chem. Soc.* **1991**, *113*, 9696].

I. Introduction

Recently, there has been considerable interest in the dynamics and kinetics of gas-phase S_N2 nucleophilic substitution reactions.[1-27] These reactions are characterized by a potential energy surface with a central barrier which separates pre- and postreaction ion–dipole complexes. The model proposed by Brauman and co-workers,[28-32] in which an ion–molecule capture theory[33] is used to calculate the association rate constant for forming the prereaction complex and Rice–Ramsperger–Kassel–Marcus (RRKM) theory[34-38] is used to calculate lifetimes for the complex, has been very successful in interpreting the kinetics of many gas-phase S_N2 reactions.[11,32] However, recent experimental[5,7,8] and theoretical[18-27] work indicates that this statistical model may be incomplete and dynamics may have to be included for some S_N2 reactions.

One S_N2 reaction, for which experimental results appear to be inconsistent with the above statistical model, is

$$Cl^- + CH_3Br \rightarrow ClCH_3 + Br^- \qquad (1)$$

Graul and Bowers[8] found relative translational energies between the reaction products $ClCH_3 + Br^-$ to be much smaller than the prediction of orbiting transition state/phase space theory (OTS/PST),[39] which assumes statistical energy partitioning at the orbiting transition state[40] for dissociation of the postreaction complex $ClCH_3$---Br^-. Viggiano et al.[7] measured the rate of

* Abstract published in *Advance ACS Abstracts*, September 15, 1994.

(1) Barlow, S. E.; Van Doren, J. M.; Bierbaum, V. M. *J. Am. Chem. Soc.* **1988**, *110*, 7240.
(2) Van Doren, J. M.; Depuy, C. H.; Bierbaum, V. M. *J. Phys. Chem.* **1989**, *93*, 1130.
(3) DePuy, C. H.; Gronert, S.; Mullin, A.; Bierbaum, V. M. *J. Am. Chem. Soc.* **1990**, *112*, 8650.
(4) Gronert, S.; Depuy, C. H.; Bierbaum, V. M. *J. Am. Chem. Soc.* **1991**, *113*, 4009.
(5) Viggiano, A. A.; Morris, R. A.; Dale, F.; Pauson, J. F.; Giles, K.; Smith, D.; Su, T. *J. Chem. Phys.* **1990**, *93*, 1149.
(6) Viggiano, A. A.; Paschkewitz, J. S.; Morris, R. A.; Paulson, J. F.; Gonzalez-Lafont, A.; Truhlar, D. G. *J. Am. Chem. Soc.* **1991**, *113*, 9404.
(7) Viggiano, A. A.; Morris, R. A.; Paschkewitz, J. S.; Paulson, J. F. *J. Am. Chem. Soc.* **1992**, *114*, 10477.
(8) (a) Graul, S. T.; Bowers, M. T. *J. Am. Chem. Soc.* **1991**, *113*, 9696. (b) Graul, S. T.; Bowers, M. T. *J. Am. Chem. Soc.* **1994**, *116*, 3875.
(9) Cyr, D. M.; Posey, L. A.; Bishea, G. A.; Han, C.-C.; Johnson, M. A. *J. Am. Chem. Soc.* **1991**, *113*, 9697.
(10) Cyr, D. M.; Bishea, G. A.; Scarton, M. G.; Johnson, M. A. *J. Chem. Phys.* **1992**, *97*, 5911.
(11) Wladkowski, B. D.; Lim, K. F.; Allen, W. D.; Brauman, J. I. *J. Am. Chem. Soc.* **1992**, *114*, 9136.
(12) Giles, K.; Grimsrud, E. P. *J. Phys. Chem.* **1992**, *96*, 6680.
(13) Strode, K. S.; Grimsrud, E. P. Submitted for publication.
(14) Knighton, W. B.; Bognar, J. A.; O'Connor, P. M.; Grimsrud, E. P. *J. Am. Chem. Soc.* **1993**, *115*, 12079.
(15) Tucker, S. C.; Truhlar, D. G. *J. Phys. Chem.* **1989**, *93*, 8138.
(16) Tucker, S. C.; Truhlar, D. G. *J. Am. Chem. Soc.* **1990**, *112*, 3338.
(17) Tucker, S. C.; Truhlar, D. G. *J. Am. Chem. Soc.* **1990**, *112*, 3347.
(18) Vande Linde, S. R.; Hase, W. L. *J. Am. Chem. Soc.* **1989**, *111*, 2349.
(19) Vande Linde, S. R.; Hase, W. L. *J. Phys. Chem.* **1990**, *94*, 2778.
(20) Vande Linde, S. R.; Hase, W. L. *J. Phys. Chem.* **1990**, *94*, 6148.
(21) Vande Linde, S. R.; Hase, W. L. *J. Chem. Phys.* **1990**, *93*, 7962.
(22) Cho, Y. J.; Vande Linde, S. R.; Zhu, L.; Hase, W. L. *J. Chem. Phys.* **1992**, *96*, 8275.
(23) Hase, W. L.; Cho, Y. J. *J. Chem. Phys.* **1993**, *98*, 8626.
(24) Billing, G. D. *Chem. Phys.* **1992**, *159*, 109.
(25) Basilevsky, M. V.; Ryaboy, V. M. *Chem. Phys. Lett.* **1986**, *129*, 71.
(26) Ryaboy, V. M. *Chem. Phys. Lett.* **1989**, *159*, 371.
(27) Ryaboy, V. M. In *Dynamics of Ion–Molecule Complexes*; Hase, W. L., Ed.; Advances in Classical Trajectory Methods, Vol. 2.; JAI Press: Greenwich, CT, 1993.
(28) Pellerite, M. J.; Brauman, J. I. *J. Am. Chem. Soc.* **1980**, *102*, 5993.
(29) Pellerite, M. J.; Brauman, J. I. *J. Am. Chem. Soc.* **1983**, *105*, 2672.
(30) Dodd, J. A.; Brauman, J. I. *J. Am. Chem. Soc.* **1984**, *106*, 5356.
(31) Dodd, J. A.; Brauman, J. I. *J. Phys. Chem.* **1986**, *90*, 3559.
(32) Moylan, C. R.; Brauman, J. I. In *Dynamics of Ion-Molecule Complexes*; Hase, W. L., Ed.; Advances in Classical Trajectory Methods, Vol. 2.; JAI Press: Greenwich, CT, 1993.
(33) Hase, W. L.; Wardlaw, D. M. In *Biomolecular Collisions*; Ashfold, M. N. R., Baggot, J. E., Ed.; Royal Society of Chemistry: London, 1989.
(34) Forst, W. *Theory of Unimolecular Reactions*; Academic Press: New York, 1973.
(35) Robinson, P. J.; Holbrook, K. A. *Unimolecular Reactions*; John Wiley & Sons: New York, 1972; p 128.
(36) Steinfeld, J. I.; Francisco, J. S.; Hase, W. L. *Chemical Kinetics and Dynamics*; Prentice Hall: Englewood Cliffs, NJ, 1989.
(37) Gilbert, R. G.; Smith, S. C. *Theory of Unimolecular and Recombination Reactions*; Blackwell: Boston, 1990.
(38) Hase, W. L. In *Dynamics of Molecular Collisions*; Miller, W. H., Ed.; Plenum: New York, 1976; Part B, p 121.
(39) Light, J. C. *Discuss. Faraday Soc.* **1967**, *44*, 14. Klots, C. E. *J. Phys. Chem.* **1971**, *75*, 1526. Klots, C. E. *Z. Naturforsch., Teil A* **1972**, *27*, 553.
(40) Chesnavich, W. J.; Bowers, M. T. In *Gas Phase Ion Chemistry*; Bowers, M. T., Ed.; Academic Press: New York, 1979.

0002-7863/94/1516-9644$04.50/0

Table 1. Geometries and Energies for Stationary Points on PES1(Br)[a]

internal coordinates	$Cl^- + CH_3Br$ reactants	$Cl^-\cdots CH_3Br$ complex	$[Cl\cdots CH_3\cdots Br]^-$ saddlepoint	$ClCH_3\cdots Br^-$ complex	$ClCH_3 + Br^-$ products
r_{C-Cl}	∞	3.221	2.470	1.819	1.789
r_{C-Br}	1.944	1.991	2.462	3.527	∞
r_{C-H}	1.077	1.071	1.062	1.074	1.077
ϕ_{H-C-Cl}	72.4	72.9	87.4	108.1	108.1
ϕ_{H-C-Br}	107.6	107.1	92.6	71.9	71.9
θ_{H-C-H}	111.3	111.5	119.8	111.8	110.8
potential energy	0	−10.731	−2.785	−21.209	−12.647

[a] Distances are in Å, angles are in deg, and energies are in kcal/mol.

Table 2. Harmonic Vibrational Frequencies for Stationary Points on PES1(Br)[a]

vibrational mode	$Cl^- + CH_3Br$ reactants	$Cl^-\cdots CH_3Br$ complex	$[Cl\cdots CH_3\cdots Br]^-$ saddlepoint	$ClCH_3\cdots Br^-$ complex	$ClCH_3 + Br^-$ products
A_1, C–H str	3048	3147[d]	3215	3101	3050
A_1, CH_3 def	1497	1467	1185	1548	1550
A_1, C–Br str[b]	620	500	161	68	
A_1, C–Cl str[b]		91	400i	646	739
E, C–H str	3183	3293	3415	3238	3181
E, CH_3 def	1457	1452	1340	1462	1460
E, CH_3 rock	1065	1089	1155	1123	1108
E, Cl^- (or Br^-) bends[c]		72	169	64	

[a] The vibrational frequencies are in units of cm^{-1}. [b] At the saddlepoint the C–Br and C–Cl stretches become a symmetric Cl–C–Br stretch and an asymmetric Cl–C–Br stretch with an imaginary frequency. [c] This mode is a Cl–C–Br bend at the saddlepoint. [d] This frequency is given incorrectly as 3047 cm^{-1} in ref 41.

reaction 1 versus reagent relative translational energy and CH_3-Br temperature. For a fixed relative translational energy, they found the rate constant does not depend on the temperature of CH_3Br, a result inconsistent with RRKM theory. This is because RRKM theory predicts that the ratio of the rate constants for $Cl^-\cdots CH_3Br$ decomposition to $Cl^- + CH_3Br$ and $ClCH_3 + Br^-$ varies with CH_3Br temperature (i.e., vibrational/rotational energy). The rate of reaction 1 has been measured versus pressure,[14] which provides insight into the lifetime of the $Cl^-\cdots CH_3Br$ complex.

In the work reported here, a multidimensional analytic potential energy function, recently developed for reaction 1,[41] is used in a classical trajectory study of the intramolecular and unimolecular dynamics associated with the $Cl^-\cdots CH_3Br$ and $ClCH_3\cdots Br^-$ complexes. Trajectories are initialized in the $Cl^-\cdots CH_3Br$ complex region of the potential energy surface with a total energy approximately characteristic of complexes formed by $Cl^- + CH_3$-Br collisions at 300 K. Different internal energy distributions are considered for the $Cl^-\cdots CH_3Br$ complex to determine whether the nature of the modes initially excited affects the chemical dynamics. Determined from the trajectories are the lifetimes of the $Cl^-\cdots CH_3Br$ and $ClCH_3\cdots Br^-$ complexes, the importance of central barrier recrossing, and the $ClCH_3 + Br^-$ product energies.

II. Potential Energy Function

An analytic potential energy function developed previously for the $Cl^- + CH_3Cl \rightarrow ClCH_3 + Cl^-$ reaction[19] was modified to derive a multidimensional analytic function for reaction 1.[41] Every atom and degree of freedom is treated explicitly by this latter potential function, which is written as

$$V_{total} = V_{Cl}(r_a,g_a)[1 - S_{LR}(g_a)] + V_{Br}(r_b,g_b)[1 - S_{LR}(g_b)] + V_{\phi}(r_a,g_a)[1 - S_{LR}(g_a)] + V_{\phi}(r_b,g_b)[1 - S_{LR}(g_b)] + V_{ClBr}[1 - S_{LR}(g_a)][1 - S_{LR}(g_b)] + V_{\theta}(g_a) + V_{\theta}(g_b) + V_{HC}(g) + V^a_{LR}S_{LR}(g_a) + V^b_{LR}S_{LR}(g_b) + \text{constant} \quad (2)$$

where $r_a = r_{C-Cl}$, $r_b = r_{C-Br}$, $g_a = r_a - r_b$, and $g_b = r_b - r_a$. The potential consists of the V_{Cl}, V_{Br}, V_{ϕ}, and V_{ClBr} terms for short-range interactions, the V_{θ} and V_{HC} terms for the CH_3 moiety,

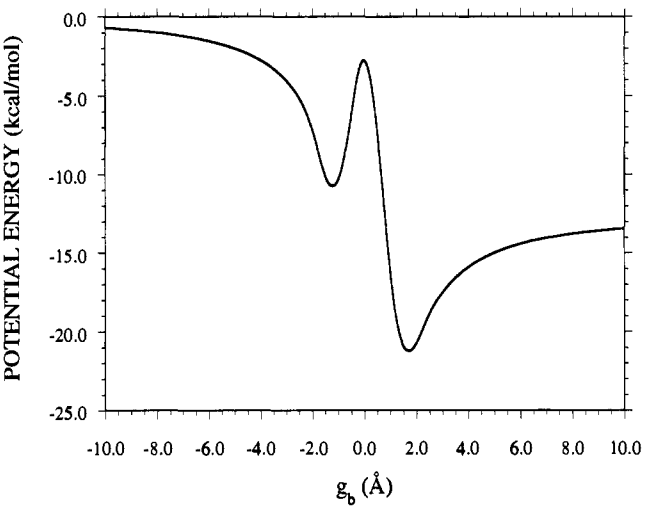

Figure 1. Reaction path potential versus $g_b = r_{C-Br} - r_{C-Cl}$ for the potential energy surface used in this work. Zero-point energy is not included in the potential energy curve. For stationary points on the potential energy surface the harmonic zero-point energy is as follows: $Cl^- + CH_3Br$ reactants, 23.70 kcal/mol; $Cl^-\cdots CH_3Br$ complex, 24.33 kcal/mol; $[Cl\cdots CH_3\cdots Br]^-$ saddle point, 23.90 kcal/mol; $ClCH_3\cdots Br^-$ complex, 24.50 kcal/mol; $ClCH_3 + Br^-$ products, 24.07 kcal/mol.

V^a_{LR} for the $Cl^- + CH_3Br$ long-range interactions, and V^b_{LR} for the $ClCH_3 + Br^-$ long-range interactions. Two sets of parameters were chosen for this analytic potential,[41] by fitting *ab initio* calculations and experimental vibrational frequencies, structures, and energies to give two potential energy surfaces identified as PES1(Br) and PES2(Br). The two surfaces only differ in their values for the H–C–Cl and H–C–Br bending force constants.[41] PES1(Br) is used for the trajectory calculations reported here.

PES1(Br) has been described in considerable detail previously[41] and only several essential features are reviewed here. Geometries and energies for stationary points on the potential energy function are listed in Table 1. Harmonic vibrational frequencies for these stationary points are listed in Table 2. The reaction path potential for PES1(Br) was determined by following the paths of steepest descent in mass-weighted Cartesian coordinates.[41] In Figure 1 the reaction path potential is plotted versus $g_b = r_{C-Br} - r_{C-Cl}$.

(41) Wang, H.; Zhu, L.; Hase, W. L. *J. Phys. Chem.* **1994**, *98*, 1608.

III. Classical Trajectory Calculations

The PES1(Br) potential energy function described above and derivatives of this potential with respect to Cartesian coordinates were incorporated into the general chemical dynamics computer program VENUS,[42] which was used for the classical trajectory calculations reported here. The trajectories were started from the prereaction complex Cl^----CH_3Br to model experiments by Graul and Bowers[8] and Cyr et al.[9] The algorithms used to select initial conditions for the complex are standard options in VENUS and have been described in considerable detail elsewhere.[43]

In the trajectory calculations different initial non-random energy distributions were investigated for the Cl^----CH_3Br complex at a total energy approximately 2.7 kcal/mol above the $Cl^- + CH_3Br$ reactants asymptotic potential, which corresponds to approximately 13.4 kcal/mol of energy in the Cl^----CH_3Br complex. From the classical potential energies in Table 1 and using the harmonic frequencies in Table 2, the total energy available to the $ClCH_3 + Br^-$ products is then approximately 15.6 kcal/mol. The average thermal rotational energy at 300 K was included in the initial energy of Cl^----CH_3Br by adding $^1/_2RT$ to each principal axis of rotation. This corresponds to a total angular momentum of $91\hbar$. A single normal mode of Cl^----CH_3Br is excited for the initial conditions investigated here. For initial conditions in which zero-point energy is not added to Cl^----CH_3Br, the energy for the excited normal mode is distributed randomly between potential and kinetic energy by choosing a random phase for the normal mode.[43]

If zero-point energy is first added to Cl^----CH_3Br, the procedure used to add vibrational energy to the complex depends on whether a CH_3Br intramolecular mode or Cl^----CH_3Br intermolecular mode is excited. As described in previous work,[22] the normal mode model is sufficiently accurate for adding zero-point energy to Cl^----CH_3Br and exciting a CH_3Br intramolecular mode. As described above, in this model the energy for a normal mode is distributed randomly between potential and kinetic by choosing a random phase for the normal mode. However, the three intermolecular modes of the Cl^----CH_3Br complex (i.e., one stretching and two bendings) are very anharmonic with low frequencies, and the above normal mode model, in which both potential and kinetic energies are added with random phase, is not sufficiently accurate for exciting an intermolecular mode with 13.4 kcal/mol of energy when zero-point energy is added. To overcome this problem, only kinetic energy was initially added when exciting an intermolecular normal mode by adding either positive or negative momentum to the mode. In this manner, the problem with anharmonicity was avoided and the normal mode model was maintained for studying selective initial excitation of the intermolecular modes. When exciting the intermolecular modes in this fashion, zero-point energy was added to the CH_3Br intramolecular modes with random phases as discussed above. Finally, when exciting two degenerate E modes like Cl^----C bending, equal amounts of quanta are added to each of the degenerate modes.

The trajectories were numerically integrated with combined fourth-order Runge–Kutta and sixth-order Adams–Moulton algorithms. An integration step size of 5×10^{-17} s was used to ensure energy conservation to 5–6 significant numbers. The integration time limit for a single trajectory was set to 2.5×10^{-11} s (i.e. 25 ps). Either 50 or 100 trajectories were integrated for each specific mode excitation.

The trajectories were analyzed for product $ClCH_3 + Br^-$ vibrational, rotational, and relative translational energies, lifetimes of the Cl^----CH_3Br and $ClCH_3$---Br^- complexes, and $[Cl$---CH_3---$Br]^-$ central barrier crossings. Each trajectory was initialized in the Cl^----CH_3Br well and the time (i.e., lifetime) the trajectory remained in this well was recorded. If the trajectory dissociated to $Cl^- + CH_3Br$ reactants, the lifetime was taken as the time of the last inner turning point in the $Cl^- + CH_3Br$ relative motion before dissociation. For isomerization to $ClCH_3$---Br^-, the lifetime was taken as the time the trajectory passed the central barrier, where $g_a = r_a - r_b$ is given by $g_a^\ddagger = 0.0112$ Å. Once the central barrier was crossed the trajectory was analyzed to determine whether it proceeded directly to $ClCH_3 + Br^-$ products, without an inner turning point in the $ClCH_3 + Br^-$ relative motion. If not, the lifetime of the resulting $ClCH_3$---Br^- complex was recorded as described above for the Cl^----CH_3Br complex.

IV. RRKM, PST, and OTS/PST Calculations

To assist in interpreting the trajectory results, RRKM theory[34-38] was used to calculate the unimolecular rate constants for the Cl^----CH_3Br and $ClCH_3$---Br^- complexes, and OTS/PST theory[39,40] was used to calculate the rate constant for $ClCH_3$---$Br^- \rightarrow ClCH_3 + Br^-$ dissociation and the $ClCH_3 + Br^-$ product energy partitioning. The vibrator transition state model was used for the RRKM calculations.[47] The rotational degree of freedom associated with the K quantum number is assumed to be active so that the RRKM rate constant is written as[46,48,49]

$$k(E,J) = \frac{\sum_{K=-J}^{J} N^\ddagger[E - E_0 - E_r^\ddagger(J,K)]}{h\sum_{K=-J}^{J} \rho[E - E_r(J,K)]} \qquad (3)$$

where E_0 is the potential energy of the transition state and E_r is the symmetric top rotational energy. The variational version of RRKM theory[51] is used to calculate the transition state properties for Cl^----$CH_3Br \rightarrow Cl^- + CH_3Br$ and $ClCH_3$---Br^- $ClCH_3 + Br^-$ dissociation. The path of steepest descent in mass-weighted Cartesian coordinates[52] and reaction path Hamiltonian[53,54] were used to find properties along the reaction paths for these dissociations. The variational transition state, for the Cl^----$CH_3Br \rightleftarrows ClCH_3$---$Br^-$ isomerizations, is located at the saddle point for the central barrier. For the energy and angular momentum considered in this work (see the previous section), the harmonic RRKM rate constants are the following: $k_{dis} = 0.3$ ps^{-1} for Cl^----$CH_3Br \rightarrow Cl^- + CH_3Br$; $k_{isom} = 0.006$ ps^{-1} for Cl^----$CH_3Br \rightarrow ClCH_3$---$Br^-$; $k_{dis} = 2$ ps^{-1} for $ClCH_3$---$Br^- \rightarrow ClCH_3 + Br^-$; and $k_{isom} = 0.0005$ ps^{-1} for $ClCH_3$---$Br^- \rightarrow Cl^-$---CH_3Br. The average lifetime for a complex is the inverse of the sum of its k_{dis} and k_{isom} rate constants. The resulting RRKM lifetimes of the pre- and postreaction complexes are 3 and 0.5 ps, respectively. Preliminary calculations[55] indicate that anharmonicity may lower these rate constants by as much as a factor of five.

A flexible transition state model[56-60] has also been used in variational RRKM calculations. For Cl^----$CH_3Cl \rightarrow Cl^- + CH_3Cl$ dissociation at 300 K, a calculation of this type, which implicitly includes a consideration of the variation of the reaction coordinate away from the center-of-mass separation distance, gives the same rate constant as determined with the vibrator/reaction path variational RRKM calculation performed here.[61] In addition, for $Cl^- + CH_3Br \rightarrow Cl^-$---$CH_3Br$ association in the temperature range of 100–1000 K, the vibrator/reaction path variational model of eq 3 gives rate constants nearly the same[41] as those determined with the statistical adiabatic channel model (SACM),[62] the orbiting transition state microcanonical variational transition state model,[63] and the trajectory capture model.[64] Thus, the vibrator/reaction path

(42) Hase, W. L.; Duchovic, R. J.; Hu, X.; Lim, K. F.; Lu, D.-h.; Swamy, K. N.; Vande Linde, S. R.; Wolf, R. J. *VENUS*, to be submitted to the Quantum Chemistry Program Exchange. *VENUS* is an enhanced version of *MERCURY*: Hase, W. L. *QCPE* **1983**, *3*, 453. Until *VENUS* is submitted to QCPE, interested parties can receive a copy of *VENUS* by contacting the authors.

(43) Sloane, C. S.; Hase, W. L. *J. Chem. Phys.* **1977**, *66*, 1523. Hase, W. L.; Ludlow, D. M.; Wolf, R. J.; Schlick, T. J. *J. Phys. Chem.* **1981**, *85*, 958.

(44) Zhu, L.; Hase, W. L. *Chem. Phys. Lett.* **1990**, *175*, 117.

(45) Aubanel, E. E.; Wardlaw, D. M.; Zhu, L.; Hase, W. L. *Int. Rev. Phys. Chem.* **1991**, *10*, 249.

(46) Zhu, L.; Chen, W.; Hase, W. L.; Kaiser, E. W. *J. Phys. Chem.* **1993**, *97*, 311.

(47) The calculations were performed with a general RRKM computer program; Zhu, L.; Hase, W. L., submitted to the Quantum Chemistry Program Exchange.

(48) Quack, M.; Troe, J. *Ber. Bunsenges. Phys. Chem.* **1974**, *78*, 240.

(49) Miller, W. H. *J. Am. Chem. Soc.* **1979**, *101*, 6820.

(50) Steinfield, J. I. *Molecules and Radiation*; MIT Press: London, 1985.

(51) Hase, W. L. *Acc. Chem. Res.* **1983**, *16*, 258.

(52) Fukui, K. *J. Phys. Chem.* **1970**, *74*, 4161.

(53) Miller, W. H.; Handy, N. C.; Adams, J. E. *J. Chem. Phys.* **1980**, *72*, 99.

(54) Kato, S.; Morokuma, K. *J. Chem. Phys.* **1980**, *73*, 3900. Morokuma, K.; Kato, S. In *Potential Energy Surface and Dynamics Calculations*; Truhlar, D. G., Ed.; Plenum Press: New York, 1981; p 243.

(55) Peslherbe, G. H.; Wang, H.; Hase, W. L. to be submitted for publication.

(56) Wardlaw, D. M.; Marcus, R. A. *J. Phys. Chem.* **1986**, *90*, 5383.

(57) Wardlaw, D. M.; Marcus, R. A. *Adv. Chem. Phys.* **1988**, *70*, Part I, 231.

(58) Aubanel, E. E.; Wardlaw, D. M. *J. Phys. Chem.* **1989**, *93*, 3117.

(59) Klippenstein, S. J. *J. Chem. Phys.* **1991**, *94*, 6469.

(60) Klippenstein, S. J. *J. Chem. Phys.* **1992**, *96*, 367.

(61) Klippenstein, S. J. private communication.

(62) Troe, J. *Chem. Phys. Lett.* **1985**, *122*, 425.

(63) Chesnavich, W. J.; Su, T.; Bowers, M. T. *J. Chem. Phys.* **1980**, *72*, 2641.

(64) Su, T.; Chesnavich, W. J. *J. Chem. Phys.* **1982**, *76*, 5183.

Table 3. $ClCH_3$ + Br^- Average Product Energies and Angular Momentum from PST, OTS/PST, and Classical Trajectories[a]

	PST		OTS/PST		
property[b]	atom + diatom	atom + sphere	atom + diatom	atom + sphere	trajectory
$\langle E_t \rangle$	2.9 ± 2.5	2.7 ± 2.4	3.0 ± 2.5	2.8 ± 2.4	1.4 ± 1.3
$\langle E_r \rangle$	2.9 ± 2.5	4.1 ± 2.8	2.8 ± 2.5	4.0 ± 2.8	0.87 ± 0.98
$\langle E_v \rangle$	9.8 ± 3.3	8.8 ± 3.3	9.8 ± 3.3	8.8 ± 3.3	13.3 ± 1.6
$\langle j \rangle$	42.7 ± 20.8	34.8 ± 13.3	42.4 ± 20.6	34.7 ± 13.2	16.3 ± 11.2

[a] The total product energy and angular momentum are 15.6 kcal/mol and 91$\hbar$, respectively. [b] Average energies are given in kcal/mol and angular momentum in $\hbar$. The uncertainties are one standard deviation of the distribution.

variational RRKM model used here is expected to accurately represent Cl^----CH_3Br and $ClCH_3$---Br^- dissociation.

Quantum harmonic phase space theory (PST)[39] and orbiting transition state/phase space theory (OTS/PST)[40] were used to calculate the product $ClCH_3$ + Br^- vibrational energy, E_v, rotational energy, E_r, and relative translational energy, E_t. PST and OTS/PST are statistical theories, which make different assumptions about the nature and role of the potential energy surface for the unimolecular reaction. PST assumes the reaction potential energy surface is of no importance in calculating product properties, and as a result, the available energy is distributed statistically between product translation, rotation, and vibration, given the constraints of total energy and angular momentum. Chesnavich and Bowers[40] modified PST by assuming (1) an orbiting transition state, located at the centrifugal barrier, with a statistical distribution of energy, and (2) an isotropic long-range potential, so that the centrifugal potential at this transition state is transformed to product translation. The OTS/PST calculations reported here utilize the isotropic ion–induced dipole potential

$$V(r) = -\frac{\alpha q^2}{2r^4} \tag{4}$$

where α is the polarizability of CH_3Cl and q is the charge of Br^-. The experimental value[65] of 4.43 Å^3 was used for α.

Equations have not been reported for treating an atom–symmetric top system either with PST or OTS/PST.[66] However, Chesnavich and Bowers[40] have shown that it is an excellent approximation, in product energy partitioning calculations, to represent an atom–symmetric top pair by an atom–sphere pair and this approach is used here, as it has been in another recent OTS/PST calculation for the $ClCH_3$ + Br^- products.[8b] The rotational constant for the sphere model is a geometric mean of the rotational constants for CH_3Cl. To compare with the atom–sphere model calculations, calculations were also performed for a linear triatom → diatom + atom model.

The equations used for the PST and OTS/PST calculations are listed in refs 39 and 40, respectively, and are not given here. As shown in Table 3, PST and OTS/PST give nearly identical results. The principal differences in the results for the atom + diatom and atom + sphere models are in the $ClCH_3$ rotational energy and angular momentum. This is expected, since the triatom → diatom + atom model has only two rotational degrees of freedom. As shown in Table 3, $\langle E_r \rangle$ for this model is approximately two-thirds of the value for the sphere → atom + sphere model.

The average energies in Table 3 are calculated using quantum harmonic state counting for the available energy of 15.6 kcal/mol and angular momentum of 91$\hbar$. The average energies are somewhat different if classical state counting is used for the total energy of 39.7 kcal/mol, which includes the $ClCH_3$ zero-point energy. For OTS/PST and the atom + diatom model the average values become $\langle E_v \rangle$ = 8.4 kcal/mol, $\langle E_r \rangle$ = 3.5 kcal/mol, and $\langle E_t \rangle$ = 3.7 kcal/mol, where the zero-point energy has been removed from $\langle E_v \rangle$. Of particular interest is that with this classical state counting $\langle E_t \rangle$ is 3.7 kcal/mol, instead of 3.0 kcal/mol found by quantum state counting.

It is also of interest to compare the PST and OTS/PST rate constants for $ClCH_3$---Br^- → $ClCH_3$ + Br^- dissociation with the RRKM rate constant given above. For the sphere → atom + sphere model, both the PST and OTS/PST rate constants are 0.5 ps^{-1}, while the PST and OTS/PST rate constants are 2 ps^{-1} for the triatom → atom + diatom model. In comparison, the vibrator RRKM model which treats the system as a symmetric top gives a rate constant of 2 ps^{-1}.[67] The difference between the sphere and triatom models is due to their different treatments of the reactive system's moment of inertia. For the triatom model, the moment of inertia of the complex $ClCH_3$---Br^- and the product $ClCH_3$ is that for the non-symmetric axes. For the sphere model, it is taken as the geometric mean of the three principal moments of inertia for both the complex $ClCH_3$---Br^- and the product $ClCH_3$. The moment of inertia along the symmetric axis is an order of magnitude smaller than the other two moments of inertia for $ClCH_3$ and two orders of magnitude smaller for the complex. With respect to the triatom model, using this geometric mean has the effect of lowering the rotational energy at a certain J and, thus, increasing both the sum and density of states at that J. From the comparisons of moments of inertia, it is obvious that this effect is bigger for the complex than for the product. Thus, the density of states is increased more than the sum of states, and the sphere model's rate constant becomes lower than that for the triatom model.

In their OTS/PST calculations, Graul and Bowers[8b] used a value for α, in eq 4, different than the experimental value of 4.43 Å^3 used here. They used a scaled α so that the $ClCH_3$ + Br^- collision rate calculated from the Langevin formula for ion–induced dipoles was the same as that determined from ADO theory, using the experimental polarizability. This gave a scaled α of 13.3 Å^3. Using this value of α, instead of 4.43 Å^3, has an insignificant effect on both the product energy partitioning and rate constant. This is because increasing α moves the orbiting transition state toward the product asymptotic limit, so that OTS/PST approaches PST. As shown in Table 3, with α = 4.43 Å^3 the OTS/PST and PST results are already nearly identical.

V. Trajectory Results

An ambiguity in classical trajectory simulations is the treatment of zero-point energy (ZPE) and its possible aphysical flow.[68] An approach proposed by Bowman et al.[69] and Miller et al.[70] for constraining ZPE flow in trajectory simulations may destroy classical phase space structures[71] important for classical/quantum correspondences.[72] Thus, it has been proposed[71] that the use of this approach be restricted to systems with ergodic dynamics. A second approach, proposed by Alimi et al.,[73] is applicable to van der Waals type systems, which have high and low frequency modes and modes whose character does not change during the course of the reaction. The criteria for applicability of these two approaches are not satisfied for the Cl^- + CH_3Br → $ClCH_3$ + Br^- reaction. The classical motion is not ergodic and the character of the modes does change appreciably during the course of the reaction. Thus, for this work, trajectories were calculated with and without adding ZPE to the normal modes of Cl^----CH_3Br. The calculations with ZPE added are called quasiclassical trajectories.[74] For the calculations with ZPE, $h\nu/2$ is first added

(65) Radzig, A. A.; Smirnov, b. M. *Reference Data on Atoms, Molecules, and Ions*; Springer-Verlag: Berlin, 1985.

(66) We are in the process of developing an algorithm for treating symmetric top systems in PST and OTS/PST calculations.

(67) If the complex's density of states is calculated for a symmetric top instead of a spherical top, the PST and OTS/PST rate constants for the sphere → atom + sphere model are 3.2 times larger and similar to that for the vibrator RRKM model.

(68) Hase, W. L. *J. Phys. Chem.* **1986**, *90*, 365. Lu, D.-h.; Hase, W. L. *J. Chem. Phys.* **1988**, *89*, 6723.

(69) Bowman, J. M.; Gazdy, B.; Sun, Q. *J. Chem. Phys.* **1989**, *91*, 2859.

(70) Miller, W. H.; Hase, W. L.; Darling, C. L. *J. Chem. Phys.* **1989**, *91*, 2863.

(71) Peslherbe, G. H.; Hase, W. L. *J. Chem. Phys.* **1994**, *100*, 1179.

(72) See the articles in: Hase, W. L. *Intramolecular and Nonlinear Dynamics*; Advances in Classical Trajectory Methods, Vol. 1; JAI Press: Greenwich, CT, 1992.

(73) Alimi, R.; Garcia-Vela, A.; Gerber, R. B. *J. Chem. Phys.* **1992**, *96*, 2034.

(74) Truhlar, D. G.; Muckerman, J. T. In *Atom–Molecule Collision Theory*; Bernstein, R. B., Ed.; Plenum Press: New York, 1979; p 505.

Table 4. Number of Different Events without ZPE Added to the Trajectories[a]

mode excited	vibrational energy[b]	no. of events: form reactants	form products	remain in complex A[c]	remain in complex B[d]	A → B crossings
E, Cl⁻ bend	12.35 (60)	2 (0)[e]	0 (0)[e]	48 (0)[e]	0 (0)[e]	0
A_1, C–Cl str	12.48 (48)	43 (0)	0 (0)	7 (0)	0 (0)	0
E, C–H str	12.52 (1.33)	0 (0)	0 (0)	50 (0)	0 (0)	0
A_1, C–H str	12.60 (1.40)	0 (0)	0 (0)	50 (0)	0 (0)	0
E, CH_3 rock	12.45 (4)	0 (0)	0 (0)	50 (0)	0 (0)	0
E, CH_3 def	12.45 (3)	0 (0)	0 (0)	50 (0)	0 (0)	0
A_1, CH_3 def	12.58 (3)	0 (0)	0 (0)	50 (0)	0 (0)	0
A_1, C–Br str	12.86 (9)	0 (0)	1 (1)	1 (1)	48 (21)	74

[a] A total of 50 trajectories were integrated for each initial condition. The maximum integration time for each trajectory is 25 ps. [b] Energies are in units of kcal/mol. Numbers in parentheses are the number of quanta added to the mode. In most cases, integral quanta were added to maintain the total energy (vibration + rotation) approximately 2.7 kcal/mol above that of reactants'. For the C–H stretching E and A modes, the frequencies are sufficiently high that fractional quanta were added to fulfill the energy requirement. [c] A is the Cl^----CH_3Br complex. [d] B is the $ClCH_3$---Br^- complex. [e] The number in parentheses is the number of trajectories of this type that have multiple crossings of the central barrier. A trajectory with an A → B crossing followed by a B → A crossing has multiple crossings.

Table 5. Number of Different Events for Quasiclassical Trajectories[a]

mode excited	vibrational energy[b]	no. of events: form reactants	form products	remain in complex A[c]	remain in complex B[d]	A → B crossings
E, Cl⁻ bend	12.35 (60)	88 (0)[e]	2 (0)[e]	6 (1)[e]	4 (1)[e]	8
A_1, C–Cl str	12.48 (48)	100 (0)	0 (0)	0 (0)	0 (0)	0
E, C–H str	12.52 (1.33)	4 (3)	17 (4)	15 (6)	64 (31)	159
A_1, C–H str	12.60 (1.40)	2 (1)	17 (13)	8 (3)	73 (29)	183
E, CH_3 rock	12.45 (4)	3 (3)	26 (12)	13 (4)	58 (26)	169
E, CH_3 def	12.45 (3)	1 (1)	23 (16)	10 (5)	66 (33)	191
A_1, CH_3 def	12.58 (3)	5 (4)	25 (16)	13 (6)	57 (25)	164
A_1, C–Br str	12.86 (9)	1 (1)	28 (23)	8 (8)	63 (44)	236

[a] A total of 100 trajectories were integrated for each initial condition. The maximum integration time for each trajectory is 25 ps. Footnotes *b–e* are the same as those in Table 4.

to each mode of Cl^----CH_3Br, and then $^3/_2RT$ thermal rotational energy and the mode specific vibrational excitation is added. For the calculations without ZPE, no zero-point energy is added to Cl^----CH_3Br before adding the rotational energy and vibrational excitation. The total harmonic ZPE of Cl^----CH_3Br is 24.33 kcal/mol.

A. Without ZPE. Listed in Table 4 are the numbers of different events observed when ZPE is not added in the trajectory initial conditions. Most of the trajectories remain in the Cl^----CH_3Br complex. For the C–H stretch, CH_3 rock, and CH_3 deformation excitations all the trajectories remain in this complex. Extensive reaction is only observed for the Cl^----C stretch intermolecular mode and C–Br stretch intramolecular mode excitations. Exciting the Cl^----C stretch intermolecular mode causes most of the complexes to dissociate to Cl^- + CH_3Br reactants. In contrast, exciting the C–Br stretch intramolecular mode leads to extensive Cl^----CH_3Br → $ClCH_3$---Br^- isomerization. It is this excitation that leads to the single reactive event out of 400 total trajectories.

The results in Table 4 show that without ZPE excitation the trajectory results are highly non-statistical and very mode specific. In some respects these results are not surprising, for without adding zero-point energy the density of states for the energy considered here is very small and much less than the quantum mechanical density of states.[35] In the next section quasiclassical trajectory results are presented, for which ZPE is added to the Cl^----CH_3Br complex. This has the effect of increasing the total classical energy, which previous studies[75] have shown tends to increase the coupling between modes and decrease the extent of mode specific dynamics.

B. With ZPE. 1. Types of Trajectory Events. The different types of events observed in the trajectories with ZPE added to Cl^----CH_3Br are enumerated in Table 5. When either the Cl^----C stretch or bend intermolecular modes are excited, the predominate event is dissociation to the reactants Cl^- + CH_3Br. The trajectories, which go to products, are direct events and do not recross the central barrier. In contrast, when the intramolecular modes of CH_3Br are excited, dissociation to form Cl^- + CH_3Br becomes unimportant. Instead, the majority of the trajectories remain in the postreaction $ClCH_3$---Br^- potential energy well after 25 ps of intramolecular motion. This is a substantial non-RRKM result. The RRKM calculations presented in the previous section, for the energy and angular momentum considered here, give lifetimes of 3 and 0.5 ps for the Cl^----CH_3Br and $ClCH_3$---Br^- complexes, respectively.

The above results show that the type of unimolecular and intramolecular dynamics exhibited by the Cl^----CH_3Br complex is differentiated by whether the intermolecular or intramolecular modes are initially excited. That this result does not depend on the specific inter- or intramolecular mode excited is rather strong evidence that one can identify two distinct types of Cl^----CH_3Br ion–dipole complexes, which are called *intermolecular* and *intramolecular complexes*.[22]

With the CH_3Br intramolecular modes of the Cl^----CH_3Br complex initially excited, an important feature of the trajectories is the multiple crossings of the central barrier. As an example, nearly one-half of these trajectories, which remain in the postreaction $ClCH_3$---Br^- complex B, have multiple central barrier crossings. For this to occur there must be at least three crossings: i.e. A → B, B → A, and then A → B. If the trajectories were integrated for longer than 25 ps, even more crossings would be expected to occur before the Cl^- + CH_3Br reactants or $ClCH_3$ + Br^- products are ultimately formed. The occurrence of these multiple crossings is a non-RRKM result, since the above RRKM calculations show that the $ClCH_3$---Br^- complex should preferentially dissociate to $ClCH_3$ + Br^- products. The ratio of products/(A → B crossings) is 0.12 for all the intramolecular mode excitation trajectories. If the trajectories were integrated for more than 25 ps, so that each trajectory attained either the reactant or product asymptotic limit, the products/(A → B crossings) ratio may change. RRKM theory predicts 2/2.006 ~ 1 for this ratio. It is unlikely that including anharmonicity in the RRKM calculations for $ClCH_3$---Br^- would decrease this ratio. Anharmonicity should be more important for the variational

(75) Lu, D.-h.; Hase, W. L. *J. Chem. Phys.* **1989**, *91*, 7490.

Table 6. Lifetimes of the Ion–Dipole Complexes for Quasiclassical Trajectories[a]

		initial Cl^----CH_3Br		Cl^----CH_3Br after recrossing(s)		$ClCH_3$---Br^-	
mode excited	energy	diss[b]	isom[c]	diss[b]	isom[c]	diss[d]	isom[e]
E, Cl^- bend	12.35(60)	1.8	9.2		10.8	9.5	1.3
A_1, C–Cl str	12.48(48)	0.005					
E, C–H str	12.52 (1.33)	15.5	8.5	3.4	0.6	6.8	2.2
A_1, C–H str	12.60 (1.40)	16.8	7.2	5.3	0.8	8.3	2.8
E, CH_3 rock	12.45 (4)		8.4	4.2	0.5	8.0	2.3
E, CH_3 def	12.45 (3)		6.8	2.7	0.4	8.1	2.2
A_1, CH_3 def	12.58 (3)	11.9	7.2	7.5	0.6	8.1	2.2
A_1, C–Br str	12.86 (9)		0.2	0.2	0.8	9.6	2.4

[a] Lifetimes are in units of ps. [b] Dissociation to Cl^- + CH_3Br. [c] Isomerization to $ClCH_3$---Br^-. [d] Dissociation to $ClCH_3$ + Br^-. [e] Isomerization to Cl^----CH_3Br.

dissociation transition state than for the transition state at the central barrier, since the former is looser with lower frequencies and contains more internal energy.[76] This would make the RRKM ratio for products/(A → B crossings) even closer to unity.

In previous work,[22] it has been suggested that the origin of such central barrier recrossings in S_N2 reactions is weak coupling between intermolecular and intramolecular complexes. The intermolecular complex is strongly coupled to the dissociation channel, while the intramolecular complex can access the central barrier. That $ClCH_3$---Br^- does not preferentially dissociate to $ClCH_3$ + Br^- products, but recrosses the central barrier, is strong evidence that there are both intramolecular and intermolecular $ClCH_3$---Br^- complexes. Thus, central barrier recrossings arise from transitions between the Cl^----CH_3Br and $ClCH_3$---Br^- intramolecular complexes. A statistical model for these transitions would predict that the ratio $ClCH_3$---Br^-/Cl^----CH_3Br equals the ratio of the densities of states for the $ClCH_3$ and CH_3Br intramolecular modes. This ratio is 4.4 for the total energy of the trajectories, and it is similar to the ratio of $ClCH_3$---Br^- and Cl^----CH_3Br complexes which remain when the trajectories with initial Cl^----CH_3Br intramolecular mode excitations are halted after 25 ps of motion. The results in Table 4 give 6 for this latter ratio.

With intramolecular mode excitations, approximately 40% of the trajectories which form products do so directly, with only one A → B barrier crossing. The remaining 60% of the reactive trajectories have at least two A → B barrier crossings. The fraction of the reactive trajectories, which are direct, is smallest for the A_1, C–Br stretch intramolecular mode excitations. This is somewhat surprising, since exciting this mode in the Cl^----CH_3-Br complex might be expected to give substantial direct substitution, as a result of the direct substitution that is observed for Cl_a^- + CH_3Cl_b collisions with C–Cl_b stretch excitation.[18,21] However, there is very little reaction and central barrier recrossings are also important, when the C–Cl_b stretch mode of the Cl_a^----CH_3-Cl_b complex is excited.[77] Clearly there are interesting questions concerning differences in the unimolecular dynamics of rotationally thermalized X^----RY complexes and those formed by X^- + RY collisions.

2. Lifetimes of the Ion–Dipole Complexes. Average trajectory lifetimes of the Cl^----CH_3Br (A) and $ClCH_3$---Br^- (B) complexes with respect to dissociation and isomerization are listed in Table 6. A distinction is made between the lifetimes of the initially formed Cl^----CH_3Br complex and that formed by B → A recrossings. In some cases the average lifetimes are rather qualitative as a result of the small number of events. To assist in analyzing the lifetimes in Table 6, it is useful to consider the above RRKM lifetimes, which are 3 ps for Cl^----CH_3Br and 0.5 ps for $ClCH_3$---Br^-. It is straightforward to show that RRKM theory predicts the same average lifetimes for isomerizing and dissociating complexes.

The dissociation and isomerization lifetimes for the initially excited Cl^----CH_3Br complex strongly depend on the mode initially excited. When the Cl^----C bend intermolecular modes are excited, the dissociation lifetime is similar to that of RRKM theory. However, exciting the Cl^----C stretch intermolecular mode gives a dissociation lifetime three orders of magnitude shorter than the RRKM prediction. When the intramolecular modes are initially excited for the Cl^----CH_3Br complex, all the isomerization lifetimes, except that for C–Br stretch excitation, are ~5 times larger than the lifetime found when the Cl^----C bend intermolecular mode is excited. Exciting the C–Br stretch intramolecular mode gives an isomerization lifetime of 0.2 ps, which is an order of magnitude shorter than the RRKM lifetime. Cl^----CH_3Br complexes formed after B → A recrossings have a much shorter lifetime for A → B isomerization than do the initially prepared Cl^----CH_3Br complexes. Thus, there appears to be a correlation in the crossings such that, after a crossing occurs, there is a tendency for an immediate recrossing. Except for the initial condition with C–Br stretch excitation, Cl^----CH_3Br complexes formed by B → A isomerization have Cl^- + CH_3Br dissociation lifetimes similar to the RRKM value.

The lifetimes for the $ClCH_3$---Br^- postreaction complex are strikingly non-RRKM. RRKM theory predicts this complex to preferentially dissociate to $ClCH_3$ + Br^- with a lifetime less than 1 ps. In contrast, the trajectory lifetime for dissociation is approximately 10 ps. The trajectory lifetime for isomerization is 1–3 ps and significantly shorter than the trajectory time for dissociation, a result inconsistent with RRKM theory.

A further analysis of the $ClCH_3$---Br^- complex lifetimes was made by plotting the natural logarithm of the relative number of these complexes versus the complex lifetime. The time the central barrier is crossed for an A → B isomerization defines $t = 0$ for the complex. An analysis of this type was done for each of the intramolecular mode excitations in Table 5 and the resulting six plots of $\ln[N(t)/N(0)]$ versus t are very similar. The two mode excitations illustrated in Figure 2 are representative, where it is seen that the plots have two time constants; i.e. $N(t)$ is biexponential. The average lifetime τ for the short-time component varies from 0.6 to 1.2 ps for the six plots, while for the long-time component the lifetime varies from 5.3 to 8.3 ps. Also plotted in Figure 2 is the RRKM prediction for $\ln[N(t)/N(0)]$, which equals $-(k_{isom} + k_{dis})t$ where k_{isom} and k_{dis} are the $ClCH_3$---Br^- → Cl^----CH_3Br and $ClCH_3$---Br^- → $ClCH_3$ + Br^- rate constants. At short time the trajectory and RRKM $N(t)$ are in approximate agreement. However, this agreement is at best fortuitous, since RRKM theory predicts dissociation to dominate, but the short-time trajectory event is isomerization (see Table 5). The unimolecular dynamics of $ClCH_3$---Br^- is strongly non-RRKM.

3. $ClCH_3$ + Br^- Product Energy Partitioning. The trajectories were analyzed for product relative translation, E_t, rotation, E_r, and vibration, E_v, energies. Average values for these product energies were statistically the same for each of the intramolecular mode excitations. Thus, the energy partitioning results for the

(76) Bhuiyan, L. B.; Hase, W. L. *J. Chem. Phys.* **1983**, *78*, 5052.
(77) Hase, W. L.; Vande Linde, S. R. unpublished results.

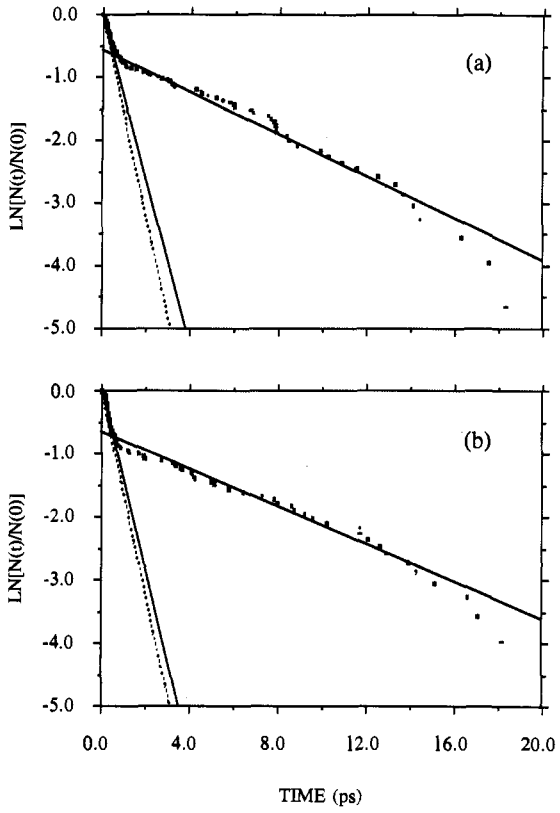

Figure 2. Relative number of $ClCH_3$---Br^- complexes versus time. The complexes are formed by Cl^----$CH_3Br \rightarrow ClCH_3$---$Br^-$ central barrier crossing and decompose by either forming the $ClCH_3 + Br^-$ products or recrossing the central barrier to form the Cl^----CH_3Br complex: (a) A_1, CH_3-deformation intramolecular mode excitation; and (b) E, CH_3-rock intramolecular mode excitation. The solid lines are the fits to the short-time and long-time decompositions. The dashed line is the RRKM prediction.

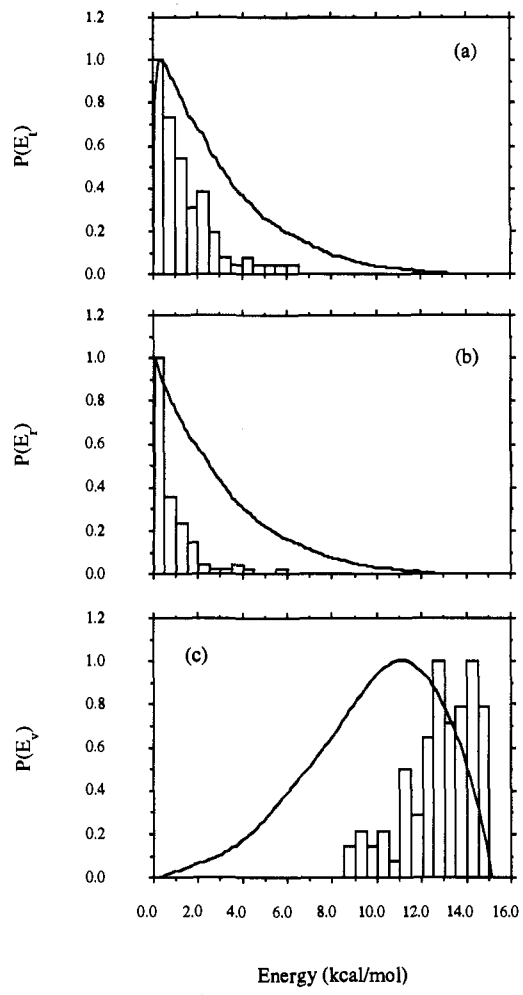

Figure 3. Product energy distributions found from the intramolecular mode excitation trajectories (histograms) and OTS/PST for the atom + sphere model (solid lines): (a) $ClCH_3 + Br^-$ relative translational energy; (b) $ClCH_3$ rotational energy; and (c) $ClCH_3$ vibrational energy.

mode excitation trajectories were combined to give the distributions in Figure 3. The average values for these distributions are $\langle E_t \rangle$ = 1.4 kcal/mol, $\langle E_r \rangle$ = 0.9 kcal/mol, and $\langle E_v \rangle$ = 13.3 kcal/mol, where $ClCH_3$ zero-point energy has been removed from the vibrational energy. The product energy is preferentially partitioned to $ClCH_3$ vibration. The $ClCH_3$ average rotational energy is approximately two-thirds of the average relative translational energy.

A comparison of the trajectory, PST, and OTS/PST average energies in Table 3 shows that PST and OTS/PST predict a higher relative translational energy and a lower vibrational energy than found from the trajectories. Product energy distributions determined by the trajectories and by OTS/PST for the atom + sphere model are compared in Figure 3.

It is worth emphasizing the significance of finding a trajectory relative translational energy distribution which is colder than that of quantum harmonic OTS/PST theory. If the trajectory dynamics were truly ergodic, the zero-point energy of the system would be free to redistribute and the total energy available for distribution in the products would be 39.7 kcal/mol. As discussed above in Section IV, classical OTS/PST theory predicts an average product relative translational energy of 3.7 kcal/mol. The energy partitioning observed from the trajectories shows that the classical motion is not ergodic and instead is approximately conserving zero-point energy for the CH_3Cl product. However, some "leak" of zero-point energy to rotation and translation is expected to occur.[68,75] As a result, a quantum dynamical calculation may give lower product relative translational energies than found from the trajectory calculations.

In their experimental study of Cl^----CH_3Br dissociation, Graul and Bowers[8] also found that the $ClCH_3 + Br^-$ product relative translational energies are less than the predictions of OTS/PST. However, a direct comparison cannot be made with their work for the following reasons: (1) the potential energy surface used in this work has a reaction exothermicity including harmonic zero-point energies of 12.27 kcal/mol, while the best experimental estimate of the exothermicity is 8–9 kcal/mol;[8] (2) the Cl^----CH_3Br complexes studied here are more energized than those of Graul and Bowers; and (3) the nature of the Cl^----CH_3Br vibrational/rotational states studied by Graul and Bowers is uncertain. An important step in making a comparison is to scale the total product energy for our trajectories and OST/PST calculations to match that of Graul and Bowers experiments, which is estimated[8] to approximately equal the reaction exothermicity. For our calculations the total product energy is 15.6 kcal/mol and, if 9 kcal/mol is assumed for the reaction exothermicity, our trajectory $\langle E_t \rangle$ = 1.4 kcal/mol should be scaled by 9/15.6 to give 0.8 kcal/mol. This number is in excellent agreement with $\langle E_t \rangle = 0.7 \pm 0.2$ kcal/mol reported by Graul and Bowers.

VI. Summary

In the work presented here classical trajectory calculations are used to study the unimolecular and intramolecular dynamics of Cl^----CH_3Br complexes excited with 13.4 kcal/mol of internal energy and 91 $\hbar$ angular momentum. Mode specific excitation is investigated in the trajectories, which are evaluated for 25 ps of internal motion. For the energy and angular momentum of the trajectories, RRKM theory predicts Cl^----CH_3Br to prefer-

entially dissociate to $Cl^- + CH_3Br$. The harmonic RRKM lifetime for Cl^----CH_3Br is 3 ps and this lifetime is only 0.5 ps for $ClCH_3$---Br^- complexes formed by Cl^----$CH_3Br \rightarrow ClCH_3$---$Br^-$ isomerization.

There are significant differences between trajectories calculated with and without ZPE added in the initial conditions. Without ZPE the reaction dynamics is highly mode specific and there is very little energy flow between modes. A similar type of dynamics was observed in trajectory studies of intramolecular vibrational energy redistribution in benzene without ZPE added.[75] The principal qualitative differences between the trajectories with and without ZPE are as follows: (1) without ZPE there is negligible energy transfer between the CH_3Br intramolecular modes of the Cl^----CH_3Br complex and central barrier crossing only occurs when the C–Br stretch mode is excited; and (2) very little $ClCH_3 + Br^-$ product formation is observed in the trajectories without ZPE. Comparisons between classical and converged quantum calculations of CH stretch relaxation in benzene[78] and linear hydrocarbon chains[79] show that there is good agreement between the classical and quantum calculations if ZPE is included in the trajectory calculations. This result suggests that, for the properties investigated here for Cl^----CH_3Br decomposition, it is more appropriate to perform the trajectories with ZPE.[80] The following are the important findings of this study for the trajectories with ZPE added:

(1) The unimolecular dynamics of the Cl^----CH_3Br complex is highly mode specific. When the low-frequency Cl^----C stretch and Cl^----CH_3Br bending modes of the complex are excited, the predominant event is dissociation to form $Cl^- + CH_3Br$. However, this is a negligible pathway when the higher frequency modes of the complex are excited. Instead, Cl^----$CH_3Br \rightarrow ClCH_3$---$Br^-$ isomerization occurs for >90% of these trajectories. The different dynamics exhibited by these two excitation patterns indicates there are two distinct types of Cl^----CH_3Br complexes, which are called intermolecular and intramolecular complexes. Experiments to study the mode specific dynamics of these two complexes are planned.[81]

(2) The trajectories, which isomerize following CH_3Br intramolecular mode excitation, do not immediately form $ClCH_3 + Br^-$ as predicted by RRKM theory. Instead the majority undergo at least one recrossing of the central barrier. After 25 ps of motion, approximately 25% of these trajectories have formed products, while more than one-half remain trapped in the $ClCH_3$---Br^- potential well. Presumably there is a substantial bottleneck for a transition from the $ClCH_3$---Br^- intramolecular to intermolecular complex and these trajectories remain in the intramolecular complex.

(3) Substantial recrossing of the central barrier is observed for trajectories with initial CH_3Br intramolecular mode excitation. The ratio of $ClCH_3 + Br^-$ product formation to Cl^----$CH_3Br \rightarrow ClCH_3$---$Br^-$ crossings (i.e. isomerizations) is approximately 0.1. This recrossing ratio may be different for other types of Cl^----CH_3Br excitations. Preliminary calculations[82] indicate that recrossings are less important than found in this work for Cl^----CH_3Br complexes formed by $Cl^- + CH_3Br$ association.

(4) The energy distributions of the $ClCH_3 + Br^-$ products formed from the trajectories are in substantial disagreement with the prediction of either PST or OTS/PST. In particular the trajectory relative translational and vibrational energies are lower and higher, respectively, than those of PST and OTS/PST. The form of the trajectory translational energy distribution is the same as measured by Graul and Bowers[8] for dissociating Cl^----CH_3Br complexes. If the reaction exothermicity of the trajectories is scaled to match that of the experiments, the theory and experimental energy distributions are nearly identical. However, the overall significance of this agreement is not clear, since it is unknown whether the experiments and trajectories are investigating the same types of dissociating states and the dependence of the product energy distribution of the nature of the dissociating state is unknown.

In conclusion, it is useful to review what is known about the nature of the dynamics which gives rise to the nonstatistical behavior observed here for $Cl^- + CH_3Br \rightarrow ClCH_3 + Br^-$ and in previous work[18-23] for $Cl_a^- + CH_3Cl_b \rightarrow Cl_aCH_3 + Cl_b^-$. Trajectories for $Cl_a^- + CH_3Cl_b \rightarrow Cl_a^-$---$CH_3Cl_b$ association show that the complex is formed by $T \rightarrow R$ energy transfer and, initially, there is no energy transfer to the CH_3Cl_b intramolecular modes, including the C–Cl_b stretch. This latter mode must become excited for the S_N2 reaction to occur and, thus, there is a dynamical bottleneck for energy transfer from the low-frequency intermolecular modes of Cl_a^----CH_3Cl_b to the higher-frequency C–Cl_b stretch. Such bottlenecks and weak couplings for energy flow have been found for numerous van der Waals systems,[83] whose potential energy surfaces are similar to those for the Cl_a^----CH_3-Cl_b, Cl^----CH_3Br, and $ClCH_3$---Br^- ion–molecule complexes. By microscopic reversibility, if there is inefficient energy transfer from the intermolecular to intramolecular modes of the complex, energy transfer will also be inefficient for the reverse process. As a result, energy may remain trapped in the intramolecular modes, with concomitant central barrier recrossings and non-RRKM dynamics, as observed in the trajectories for Cl_a^----$CH_3Cl_b \leftrightarrow Cl_aCH_3$---$Cl_b^-$ and Cl^----$CH_3Br \leftrightarrow ClCH_3$---$Br^-$. A better model for dissociation of a S_N2 complex to form ion + molecule products may be a nonstatistical vibrational predissociation mechanism,[84] instead of the statistical energy transfer associated with RRKM theory.

Additional work is currently in progress to provide more details for the above model. Of interest is the nature of the mode couplings and the phase space structure as the system descends the S_N2 central barrier and forms products (or reactants). A goal of this analysis is to determine which modes affect central barrier recrossings and contribute to couplings between the intermolecular and intramolecular ion–dipole complexes.

Acknowledgment. This research was supported by the National Science Foundation.

(78) Wyatt, R. E.; Iung, C.; Leforestier, C. *J. Chem. Phys.* **1992**, *97*, 3477.
(79) Topaler, M.; Makri, N. *J. Chem. Phys.* **1992**, *97*, 9001.
(80) If trajectory calculations are to be used to determine fine dynamical details like the structure within a CH stretch absorption band, ref 77, or lifetimes of long-lived resonance states, both of which arise from recurrences in the dynamics, it may be necessary to calculate the trajectories without or with only a small fraction of the ZPE. Including ZPE gives the broad dynamical features, but not fine structures in the dynamics. See discussions in: Lu, D.-h.; Hase, W. L. *J. Phys. Chem.* **1988**, *92*, 3217. Gomez Llorente, J. M.; Hahn, O.; Taylor, H. S. *J. Chem. Phys.* **1990**, *92*, 2762. Also ref 75.
(81) Shin, S. K. private communication.
(82) Wang, H.; Hase, W. L. to be submitted for publication.
(83) Miller, R. E. *Science* **1988**, *240*, 447.
(84) Ewing, G. E. *J. Chem. Phys.* **1980**, *72*, 2096.